Tracing the upper ocean's "missing heat"

C. A. Katsman[1] and G. J. van Oldenborgh[1]

Received 7 June 2011; accepted 15 June 2011; published 30 July 2011.

[1] Over the period 2003–2010, the upper ocean has not gained any heat, despite the general expectation that the ocean will absorb most of the Earth's current radiative imbalance. Answering to what extent this heat was transferred to other components of the climate system and by what process(-es) gets to the essence of understanding climate change. Direct heat flux observations are too inaccurate to assess such exchanges. In this study we therefore trace these heat budget variations by analyzing an ensemble of climate model simulations. The analysis reveals that an 8-yr period without upper ocean warming is not exceptional. It is explained by increased radiation to space (45%), largely as a result of El Niño variability on decadal timescales, and by increased ocean warming at larger depths (35%), partly due to a decrease in the strength of the Atlantic meridional overturning circulation. Recently-observed changes in these two large-scale modes of climate variability point to an upcoming resumption of the upward trend in upper ocean heat content. **Citation:** Katsman, C. A., and G. J. van Oldenborgh (2011), Tracing the upper ocean's "missing heat," *Geophys. Res. Lett.*, *38*, L14610, doi:10.1029/2011GL048417.

1. Introduction

[2] Observations of ocean temperature have been synthesized into global upper ocean heat content (UOHC) analyses by various groups [*Levitus et al.*, 2009; *Ishii and Kimoto*, 2009; *Domingues et al.*, 2008; *Lyman et al.*, 2010], where UOHC is defined as the integral of ocean heat content (OHC) over 0–700 m depth. Over the past eight years, all estimates show a flattening of the UOHC curve, regardless of the applied gap-filling strategies to deal with the sparseness of the data, data quality control procedures, or correction of biases in the in-situ data [*Levitus et al.*, 2009; *Ishii and Kimoto*, 2009; *Lyman et al.*, 2010]. Based on the past long-term trend, this implies that roughly $2.4 \cdot 10^{22}$ J is now "missing" from the upper ocean. As the upper ocean is thought to absorb most of the excess energy trapped by rising greenhouse gas concentrations [*Forster et al.*, 2007], such events imply substantial changes in the Earth's energy balance [*Trenberth and Fasullo*, 2010], which, despite their magnitude, are beyond our monitoring capabilities [*Trenberth*, 2009]. Observation-based arguments of *Trenberth* [2009], *Trenberth and Fasullo* [2010], and the auxiliary material rule out that the bulk of the upper ocean's "missing heat" was absorbed by the atmosphere, the land or the cryosphere, implying that most of this heat was stored deeper in the ocean and/or radiated back to space.[1]

2. Simulated OHC Changes

[3] To explore the variability in OHC and associated energy budget changes, we analyze an ensemble of 17 climate model simulations [*Sterl et al.*, 2008] performed with the ECHAM5-MPI/OM1 coupled climate model [*Roeckner et al.*, 2003; *Marsland et al.*, 2003], for the period 1950–2100 (see auxiliary material for details). Timeseries for the global mean OHC are calculated from the simulated ocean temperatures down to a specific depth. After correction for a small temperature drift (auxiliary material), the resulting timeseries of global mean UOHC (0–700 m depth) display a long-term upward trend that is very similar to the observation-based curves (Figure 1). Also the variability in the rise in UOHC is well-simulated by the ensemble. Spatially, variability around the long-term trend in global mean UOHC is associated with variations in the western Pacific Ocean and to a lesser extent in the North Atlantic Ocean, both in the observations and in the model (auxiliary material).

3. Eight-Year Trends in OHC

[4] Because of the large interannual variability (Figure 1a), the flattening of the UOHC curve is not statistically significant in the observational record [*Lyman et al.*, 2010]. The large amount of data obtained from the model ensemble does allow for a robust assessment of the probability of such an event. From the distribution of linear trends in UOHC, it appears that 11% of all overlapping 8-yr periods in the time frame 1969–1999 have a zero or negative UOHC trend (Figure 2a). Over 1990–2020, around the time of the observed flattening, this is reduced to 3% (Figure 2b), corresponding to a probability of 57% of at least one zero or negative 8-yr trend in this time frame. Below we explore the energy budget changes associated with these events by analyzing 8-yr anomalous trends in UOHC with respect to the ensemble mean trend. It appears that on average 80% of these trends can be explained by an increase in the 8-yr mean net outgoing top-of-the-atmosphere (TOA) radiation (45%) and an increase in OHC below 700 m (35%).

3.1. Radiation to Space

[5] In the model simulations, episodes with a negative anomalous 8-yr trend in UOHC are usually accompanied by an increase in the net outgoing TOA radiation (Figure 3a). About two-thirds of the anomalous upper ocean heat loss is due to extra outgoing short-wave (solar) TOA radiation, the remaining one-third is due to long-wave TOA radiation (Figure 3b). The short-wave component implies that increased reflection back to space drives part of the UOHC trend (the solar irradiation is constant in the model). The long-wave component can be seen as a delayed damping response

[1]Global Climate Division, KNMI, De Bilt, Netherlands.

[1]Auxiliary materials are available in the HTML. doi:10.1029/2011GL048417.

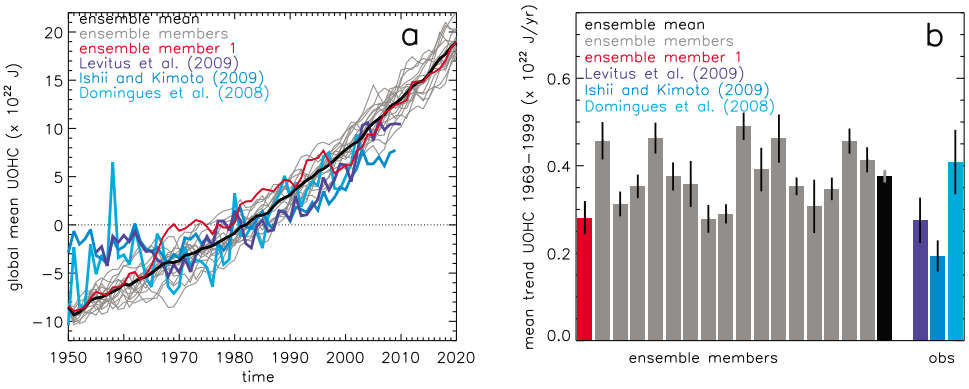

Figure 1. (a) Timeseries of changes in UOHC (0–700 m) for 1950–2020 from the model ensemble (grey, member #1 is highlighted in red, the ensemble mean is shown in black) and observations (dark blue: *Levitus et al.* [2009], blue: *Ishii and Kimoto* [2009], light blue: *Domingues et al.* [2008]) referenced to the average over 1957–2003. (b) Long-term trends in UOHC over 1969–1999, including the 2-σ uncertainty band (ensemble mean: $0.38 \pm 0.014 \cdot 10^{22}$ J yr^{-1}; individual ensemble members: 0.28 to $0.49 \cdot 10^{22}$ J yr^{-1}); observations: $0.28 \pm 0.052 \cdot 10^{22}$ J yr^{-1} [*Levitus et al.*, 2009], $0.19 \pm 0.036 \cdot 10^{22}$ J yr^{-1} [*Ishii and Kimoto*, 2009], and $0.41 \pm 0.074 \cdot 10^{22}$ J yr^{-1} [*Domingues et al.*, 2008].

(Figure 3b): an anomalous negative UOHC trend generally represents a situation that the upper ocean is warmer than the ensemble mean at first and looses more heat to the atmosphere, which increases long-wave radiation to space. Later on this reverses to lower than average radiation when the upper ocean has become cooler than the ensemble mean. The delay of about one year causes a positive contribution at zero lag (Figure 3b).

[6] The spatial pattern of net outgoing TOA radiation associated with an 8-yr rise in global mean UOHC (Figure 3c) resembles the effect of La Niña on TOA radiation over the Pacific Ocean [*Trenberth et al.*, 2002], in line with observations [*Trenberth et al.*, 2002; *Trenberth*, 2009] that the upper ocean gains heat from the atmosphere during La Niña and looses heat during El Niño. On average, the central year of a negative UOHC trend is preceded by a period dominated by El Niño events (Figure 3d), and associated with a transition to a decadal La Niña phase four to five years later.

3.2. Deep Ocean Warming

[7] In addition, at times when the 8-yr anomalous trend in UOHC is negative, the deep ocean heat content (DOHC, defined as the integral over 700–3000 m) displays a positive trend that on average compensates 35% of the upper ocean changes (Figure 4a). In part, this appears to be a response to a decreased Atlantic Meridional Overturning Circulation (AMOC). The reverse deep ocean trend is most pronounced at a depth of 1000–1500 m (Figure 4b) in the North Atlantic Ocean (Figure 4c) at latitudes where the downward limb of the AMOC is found [*Jungclaus et al.*, 2006]. In this region, deep ocean convection [*Marshall and Schott*, 1999] mixes the warm, salty waters at mid-depths with the cool, fresh surface waters, causing a reduction of the (local) DOHC [*Yashayaev and Loder*, 2009]. Although the convectively-formed water masses only contribute a small fraction of the total AMOC [*Pickart and Spall*, 2007], the intensity of

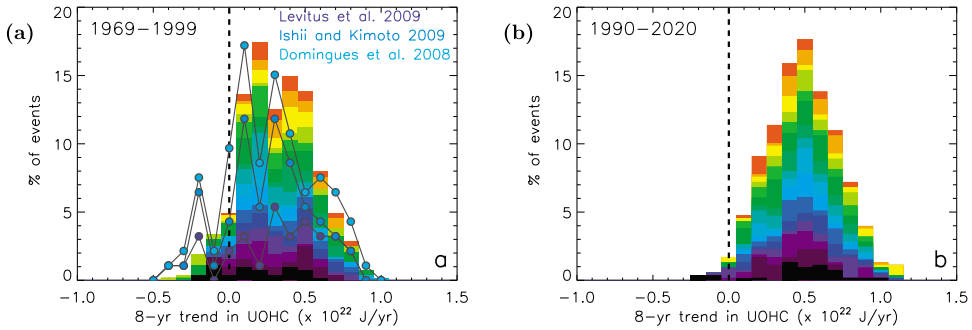

Figure 2. (a) Stacked distribution of 8-yr trends in UOHC with central years ranging from 1969–1999 (individual ensemble members are distinguished by color; the distribution is composed from 17 members × 31 overlapping 8-yr periods = 527 trend values). This time frame is the longest period over which such a distribution can also be composed from three observational datasets, omitting the uncertain UOHC estimates up to the mid-1960s when data coverage was particularly poor [*Levitus et al.*, 2009]. Although the observation-based curves (lines with dots, color-coded as in legend) are not independent realizations like the different ensemble members, their distributions are also stacked for plotting purposes. (b) As Figure 2a, for the period 1990–2020, representing the conditions around the time of the observed flattening over 2003–2010. In Figure 2a, 11% of the distribution consists of zero or negative trend values; in Figure 2b this is reduced to 3%. This corresponds to a 97% chance of at least one period with an 8-yr negative trend occurring for 1969–1999 and a 57% chance for 1990–2020.

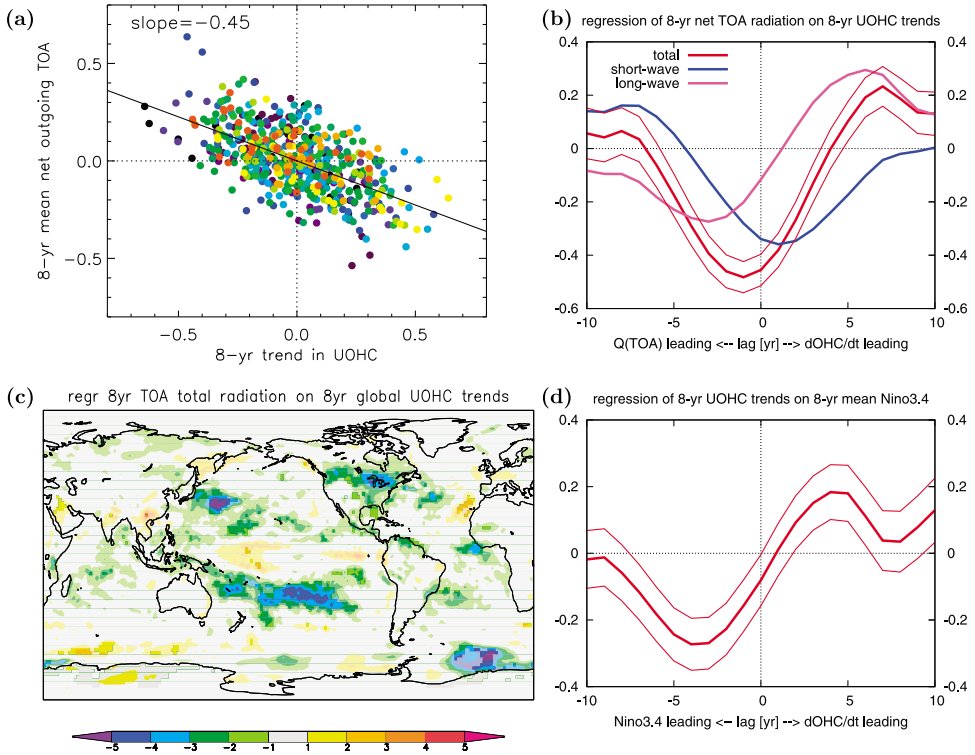

Figure 3. (a) Scatter plot of 8-yr trends in UOHC (0–700 m) and 8-yr mean net outgoing TOA radiation (in 10^{22} J yr^{-1}, global mean anomalies w.r.t. the ensemble mean, ensemble members distinguished by color). The least squares fit (black line) has a slope of −0.45 (correlation is −0.60, $p < 10^{-8}$). (b) Lagged regressions of net outgoing TOA radiation on UOHC trends (red, with 95% confidence interval), decomposed in its short-wave (solar, blue) and long-wave (thermal, magenta) components. (c) Spatial pattern of the correlation between the local outgoing TOA radiation and the global mean UOHC trends. In light shaded areas the correlation is not significant at $p < 0.05$. (d) Lagged regression of the UOHC trend on the 8-yr running mean Niño3.4-index [*Philander*, 1990], demonstrating a significant negative (positive) correlation at a lag of −7 to 0 years (2 to 6 years). All panels are for the period 1990–2020.

deep convection strongly influences the AMOC variability on decadal time scales [*Biastoch et al.*, 2008; *Eden and Willebrand*, 2001]. At times when deep convection is weak or absent in our model simulations, the AMOC presumably weakens. This yields a warming of the deeper ocean waters due to the reduced ventilation by colder surface waters (Figure 4d).

4. Recent Absence of Ocean Warming

[8] The two modes of climate variability identified in the model simulations as the main drivers for anomalous negative UOHC trends when they act in concert may also have played a role over the past eight years. During 2002–2007, a series of El Niño events occurred (www.cpc.noaa.gov/data/indices/), which probably yielded a larger than average upper ocean heat loss [*Trenberth et al.*, 2002] caused by the (lagged) response through net outgoing TOA radiation (Figure 3b). This seems at odds with direct observations that indicate an opposing increase in the radiation from space [*Trenberth and Fasullo*, 2010], but the record has large uncertainties and is too short to separate trends from decadal variability. Observations of spatially resolved net outgoing TOA radiation are not of sufficient length and accuracy to assess the verisimilitude of the modeled radiation pattern (Figure 3c) associated with the anomalous UOHC trend.

[9] Long timeseries of DOHC trends that have been corrected for instrumentation problems [*Gouretski and Koltermann*, 2007; *Wijffels et al.*, 2008; *Willis et al.*, 2009] are not available, but the observation that the OHC over 0–2000 m has risen substantially over 2003–2008 [*von Schuckmann et al.*, 2009; *Song and Colberg*, 2011] while it has reached a plateau in the upper ocean [*Lyman et al.*, 2010] supports the view that part of the "missing heat" is to be found deeper in the ocean. The uncertainty in the trend over 0–2000 m [*von Schuckmann et al.*, 2009] can easily accommodate the "missing" anomalous DOHC trend of about 35% × 0.3 · 10^{22} J yr^{-1} deduced from the model analysis (Figure 4a).

[10] The explanation that this heat exchange is linked to variability in the strength of the AMOC is compatible with observations of the convective activity in the North Atlantic Ocean. During the winters of 2001–2002 to 2006–2007, deep convection in the Labrador Sea ceased and the local ocean waters at mid-depth warmed gradually because of the lack of mixing [*Yashayaev and Loder*, 2009]. The observational record of the AMOC strength [*Cunningham et al.*, 2007; *Willis*, 2010] is too short to asses whether the lack of Labrador Sea convection caused the expected reduction of the AMOC [*Pickart and Spall*, 2007].

[11] The solar irradiation (kept constant in the model) has decreased over the past few years [*Trenberth*, 2009] but its

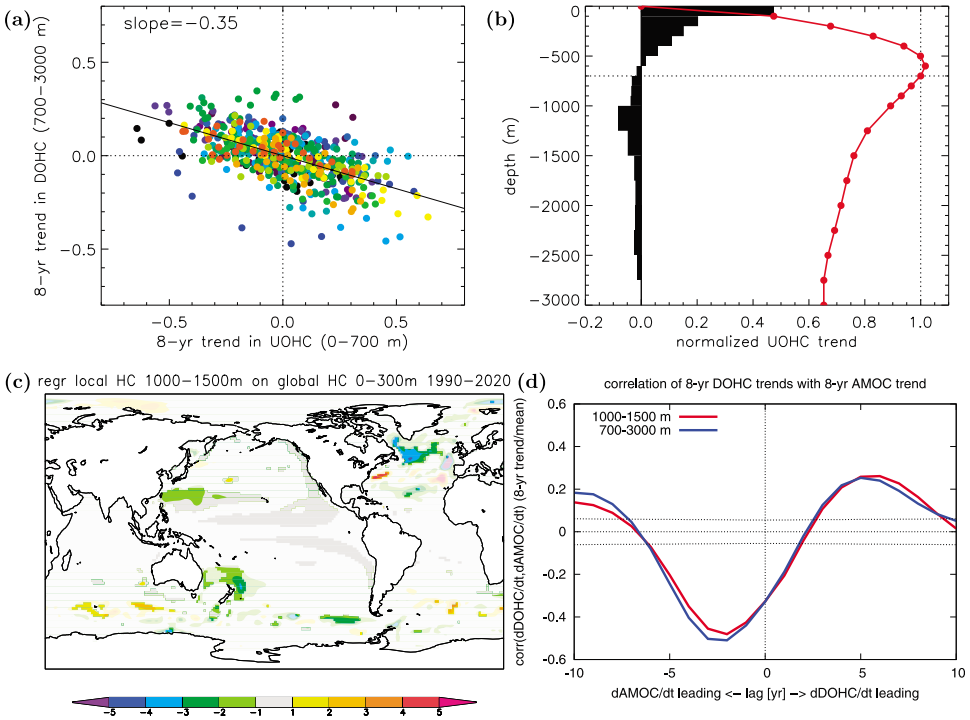

Figure 4. (a) Scatter plot for 8-yr trends in UOHC (0–700 m) and DOHC (700–3000 m) (in 10^{22} J yr^{-1}, global mean anomalies w.r.t. the ensemble mean, ensemble members distinguished by color). The least squares fit (black line) has a slope of −0.35 (correlation is −0.60, $p < 10^{-8}$). (b) Average trend in OHC normalized by the trend in UOHC (red: cumulative down from the surface, black bars: by depth interval). (c) Correlation between the global mean trend in OHC over 0–300 m and the local trend over 1000–1500 m. (d) Lag correlation between the 8-yr trend in DOHC (red: 1000–1500 m, blue: 700–3000 m, stippled lines indicate correlations with $p = 0.05$) and the 8-yr trend in the strength of the AMOC at 35° N. All panels are for the period 1990–2020.

mean value over 2003–2010 is only slightly lower than the long-term mean and can at most explain about 10% of the "missing heat" over that period [*Trenberth and Fasullo*, 2010]. The radiative effects of tropospheric aerosols were included in the ECHAM5-MPI/OM1 climate model [*Roeckner et al.*, 2003], but there is evidence that the resulting radiative response is not as strong as observed [*van Oldenborgh et al.*, 2009; *Ruckstuhl and Norris*, 2009]. However, the resulting albedo changes cannot explain the lack of increase in UOHC as the aerosol optical depth is seen to decrease on average [*Wild*, 2009].

5. Implications for the Coming Years

[12] Based on the model results, a resumption of the upward trend in UOHC is anticipated within a few years. Not only does the chance that the UOHC curve remains flat for much longer reduce quickly (auxiliary material), recently observed changes in El Niño–Southern Ocean variability and ocean convection activity also point in that direction. By the end of 2007, a transition to La Niña has occurred (www.cpc.noaa.gov/data/indices/), which is a precursor of increasing UOHC trends [*Trenberth et al.*, 2002]. Secondly, the Labrador Sea did experience deep convection again during the winter of 2007–2008 [*Vaage et al.*, 2008] and a consequent local cooling at mid-depth [*Yashayaev and Loder*, 2009], implying an increase in the strength of the AMOC [*Pickart and Spall*, 2007]. In the model, this is associated with a reduction of the global mean DOHC and an increase in UOHC two to three years later (Figure 4).

[13] **Acknowledgments.** We thank Sydney Levitus, Masayoshi Ishii, Catia Domingues and their co-workers for making available the timeseries of global mean UOHC reproduced in Figure 1, and Richard Bintanja, Wilco Hazeleger, Bart van den Hurk, and Sybren Drijfhout for discussions on the manuscript. The ESSENCE project, lead by Wilco Hazeleger (KNMI, the Netherlands) and Henk Dijkstra (Utrecht University/IMAU, the Netherlands), was carried out with support of DEISA, HLRS, SARA and NCF (through NCF projects NRG-2006.06, CAVE-06-023 and SG-06-267). We thank the DEISA Consortium (co-funded by the EU, FP6 projects 508830 / 031513) for support within the DEISA Extreme Computing Initiative (www.deisa.org). The authors thank Andreas Sterl (KNMI), Camiel Severijns (KNMI), and HLRS and SARA staff for technical support.

References

Biastoch, A., C. W. Böning, J. Getzlaff, J.-M. Molines, and G. Madec (2008), Causes of interannual-decadal variability in the meridional overturning circulation of the midlatitude North Atlantic Ocean, *J. Clim.*, *21*, 6599–6615, doi:10.1175/2008JCLI2404.1.

Cunningham, S. A., et al. (2007), Temporal variability of the Atlantic meridional overturning circulation at 26.5°N, *Science*, *317*, 935–938, doi:10.1126/science.1141304.

Domingues, C. M., J. A. Church, N. J. White, P. J. Gleckler, S. E. Wijffels, P. M. Barker, and J. R. Dunn (2008), Rapid upper-ocean warming helps explain multi-decadal sea-level rise, *Nature*, *453*, 1090–1093, doi:10.1038/nature07080.

Eden, C., and J. Willebrand (2001), Mechanism of interannual to decadal variability of the North Atlantic circulation, *J. Clim.*, *14*, 2266–2280.

Forster, P., et al. (2007), Changes in atmospheric constituents and in radiative forcing, in *Climate Change 2007: The Physical Science Basis. Contribution of Working Group I to the Fourth Assessment Report of the*

Intergovernmental Panel on Climate Change, edited by S. Solomon et al., pp. 129–234, Cambridge Univ. Press, Cambridge, U. K.

Gouretski, V., and K. P. Koltermann (2007), How much is the ocean really warming?, *Geophys. Res. Lett.*, *34*, L01610, doi:10.1029/2006GL027834.

Ishii, M., and M. Kimoto (2009), Reevaluation of historical ocean heat content variations with time-varying XBT and MBT depth bias corrections, *J. Oceanogr.*, *65*, 287–299.

Jungclaus, J. H., N. Keenlyside, M. Botzet, H. Haak, J. J. Luo, M. Latif, J. Marotzke, U. Mikolajewicz, and E. Roeckner (2006), Ocean circulation and tropical variability in the coupled model ECHAM5/MPI-OM, *J. Clim.*, *19*, 3952–3972.

Levitus, S., J. I. Antonov, T. P. Boyer, R. A. Locarnini, H. E. Garcia, and A. V. Mishonov (2009), Global ocean heat content 1955–2008 in light of recently revealed instrumentation problems, *Geophys. Res. Lett.*, *36*, L07608, doi:10.1029/2008GL037155.

Lyman, J. M., S. A. Good, V. V. Gouretski, M. Ishii, G. C. Johnson, M. D. Palmer, D. A. Smith, and J. K. Willis (2010), Robust warming of the global upper ocean, *Nature*, *465*, 334–337, doi:10.1038/nature09043.

Marshall, J., and F. Schott (1999), Open ocean deep convection: Observations, models and theory, *Rev. Geophys.*, *37*, 1–64.

Marsland, S. J., H. Haak, J. H. Jungclaus, M. Latif, and F. Roske (2003), The Max Planck Institute global ocean/sea-ice model with orthogonal curvilinear coordinates, *Ocean Modell.*, *5*, 91–127.

Philander, S. G. (1990), *El Niño, La Niña and the Southern Oscillation*, 293 pp., Academic, San Diego, Calif.

Pickart, R. S., and M. A. Spall (2007), Impact of Labrador Sea convection on the North Atlantic meridional overturning circulation, *J. Phys. Oceangr.*, *37*, 2207–2227, doi:10.1175/JPO3178.1.

Roeckner, E., et al. (2003), The atmospheric general circulation model ECHAM5. Part I: Model description, *Rep. 349*, Max Planck Inst. for Meteorol., Hamburg, Germany.

Ruckstuhl, C., and J. R. Norris (2009), How do aerosol histories affect solar "dimming" and "brightening" over Europe?: IPCC-AR4 models versus observations, *J. Geophys. Res.*, *114*, D00D04, doi:10.1029/2008JD011066.

Song, Y. T., and F. Colberg (2011), Deep ocean warming assessed from altimeters, Gravity Recovery and Climate Experiment, in situ measurements, and a non-Boussinesq ocean general circulation model, *J. Geophys. Res.*, *116*, C02020, doi:10.1029/2010JC006601.

Sterl, A., C. Severijns, H. Dijkstra, W. Hazeleger, G. Jan van Oldenborgh, M. van den Broeke, G. Burgers, B. van den Hurk, P. Jan van Leeuwen, and P. van Velthoven (2008), When can we expect extremely high surface temperatures?, *Geophys. Res. Lett.*, *35*, L14703, doi:10.1029/2008GL034071.

Trenberth, K. E. (2009), An imperative for climate change planning: Tracking Earth's global energy, *Curr. Opin. Environ. Sustainability*, *1*, 19–27, doi:10.1016/j.cosust.2009.06.001.

Trenberth, K. E., and J. T. Fasullo (2010), Tracking Earth's energy, *Science*, *328*, 316–317, doi:10.1126/science.1187272.

Trenberth, K. E., J. M. Caron, D. P. Stepaniak, and S. Worley (2002), Evolution of El Niño–Southern Oscillation and global atmospheric surface temperatures, *J. Geophys. Res.*, *107*(D8), 4065, doi:10.1029/2000JD000298.

Vaage, K., R. S. Pickart, V. Thierry, G. Reverdin, C. M. Lee, B. Petrie, T. A. Agnew, A. Wong, and M. Ribergaard (2008), Surprising return of deep convection to the subpolar North Atlantic in winter 2007–2008, *Nat. Geosci.*, *2*, 67–72,doi:10.1038/ngeo382.

van Oldenborgh, G. J., S. S. Drijfhout, A. van Ulden, R. Haarsma, A. Sterl, C. Severijns, W. Hazeleger, and H. A. Dijkstra (2009), Western Europe is warming much faster than expected, *Clim. Past*, *5*, 1–12.

von Schuckmann, K., F. Gaillard, and P.-Y. Le Traon (2009), Global hydrographic variability patterns during 2003–2008, *J. Geophys. Res.*, *114*, C09007, doi:10.1029/2008JC005237.

Wijffels, S. E., J. Willis, C. M. Domingues, P. Barker, N. J. White, A. Gronell, K. Ridgway, and J. A. Church (2008), Changing eXpendable BathyThermograph fall-rates and their impact on estimates of thermosteric sea level rise, *J. Clim.*, *21*, 5657–5672, doi:10.1175/2008JCLI2290.1.

Wild, M. (2009), Global dimming and brightening: A review, *J. Geophys. Res.*, *114*, D00D16, doi:10.1029/2008JD011470.

Willis, J. K. (2010), Can in situ floats and satellite altimeters detect long-term changes in Atlantic Ocean overturning?, *Geophys. Res. Lett.*, *37*, L06602, doi:10.1029/2010GL042372.

Willis, J. K., J. M. Lyman, G. C. Johnson, and J. Gilson (2009), In situ data biases and recent ocean heat content variability, *J. Atmos. Oceanic Technol.*, *26*, 846–852, doi:10.1175/2008JTECHO608.1.

Yashayaev, I., and J. W. Loder (2009), Enhanced production of Labrador Sea Water in 2008, *Geophys. Res. Lett.*, *36*, L01606, doi:10.1029/2008GL036162.

C. A. Katsman and G. J. van Oldenborgh, Global Climate Division, KNMI, PO Box 201, NL-3730 AE De Bilt, Netherlands. (caroline.katsman@knmi.nl)